International Journal Of Engineering Research And Development
e-ISSN: 2278-067X, p-ISSN: 2278-800X, www.ijerd.com
Volume 14, Issue 2 (February Ver. I 2018), PP.48-61

Problems of Modeling the Phase Transformations in Nonlinear and Relaxed Optics

Petro P. Trokhimchuck
Department of Theoretical and Mathematical Physics, Lesya Ukrayinka East European National University, 13 Voly Avenue, 43025, Lutsk, Ukraine,
Corresponding Author: Petro P. Trokhimchuck

ABSTRACT:- Problems of modeling the phase transformations in Nonlinear and Relaxed Optics are discussed. It was shown that these processes may be having nonequilibrium and irreversible nature. The influence of mechanisms of light scattering on formation Nonlinear and Relaxed optical processes is analyzed. Classification of proper light-induced phase transformations is represented. Cascade nature of these transformations is observed. Methods of modeling shock waves processes is used fore modeling laser-induced volume phase transformations. Corresponding experimental data are analyzed too.
KEYWORDS:- Nonlinear Optics, Relaxed Optics, phase transitions, saturation of excitation, cascade processes, irreversible phenomena, nonequilibrium phenomena

---

Date of Submission: 16 -02-2018 Date of acceptance: 03-03 2018

I. INTRODUCTION

Problem of modeling the phase transformations in Nonlinear Optics (NLO) [1, 2] and Relaxed optics (RO) [2 – 4] is very complex problem. It connected with various nature of relaxation of first-order optical excitation. For the case NLO we have radiated non-equilibrium relaxation; for RO – unradiated irreversible relaxation, which is caused the macroscopic phase transformations in irradiated matter. Therefore we must use various methods of modeling of these processes and phenomena.

Basic NLO phenomena are connected with processes of intrinsic light scattering (absorption) on stable or metastable centers. So, the concentrations these centers in solid are equaled ~ 10^{15}–10^{17} cm^{-3}. Therefore we can use adiabatic approximation and basic formalisms of NLO are perturbation theory and nonlinear differential and integral equations. According by H. Haken [1] NLO phenomena may be represented as nonequilibrium second-order phase transitions. This idea was developed in [5].

Relaxed Optics (RO) is the chapter of modern physics of irreversible interaction light and matter [2 – 4]. Necessity of creation RO is caused of technological applications of laser radiation (laser annealing, laser implantation and other [4]). Phenomenological energy-time and electromagnetic classifications of processes and phenomena of interaction light and matter are basis of RO. According to energy-time classification we have three types of processes and phenomena: kinetic (mainly quantum first-order processes); dynamic (mainly wave second-order processes) and mixing kinetic-dynamic or dynamic-kinetic processes. Properly to this concept we can have three types phase transformations: kinetic, dynamic and more complex cascade kinetic-dynamic or dynamic-kinetic processes. Really it is photochemical, plasmic, thermal and mixing phenomena [4].

Thermal and plasmic processes are the field processes and for the light scattering in matter it are second order processes. Therefore the time of formation of these processes is more as time of first-order quantum processes (photochemical or photocrystall chemical). Hierarchy of this times is next: time of optical excitation – 10^{-18} –10^{-15} s, time of local (quantum) electromagnetic relaxation – 10^{-15} –10^{-12} s, time of generation of plasmic oscillations – 10^{-13} –10^{-10} s, “thermal” times of heating and cooling – 10^{-9} –10^{-5} s [4]. First two processes are primary and quantum processes, last two processes are secondary.

Primary processes are caused of mechanisms of light scattering and local microscopic relaxation, secondary – macroscopic relaxation mechanisms. Therefore we must include these results for the explanation of real picture of interaction light and matter.

Therefore methods for modeling of the laser-induced surface and volume phase transformations are various. This fact is caused of different conditions of radiation: self-absorption for surface and intrinsic absorption for volume. In first case we may have processes of one or two photon processes and for second case – multiphotonic processes.

II. BASIC METHODS OF MODELING THE PHASE TRANSFORMATIONS AND PHASE TRANSITIONS

Firstly we must determine the notion of phase transformations and phase transitions. Phase transformations are represented change of phase state of matter. This change may be discrete and continuous. Phase transitions are physical and chemical processes, which are explained with help thermodynamic theory of phase transitions. Phase transitions is characterized the jump behavior of change the proper physical quantity [6].

Thermodynamic theory of phase transitions is based on the Erenfest classification [6]. According to this classification for case of the first-order phase transitions Gibbs potential is changed continuous but its first partial derivatives have uneven character in point of transition. For second-order phase transitions Gibbs potential and its first partial derivatives are changed continuous but its second partial derivatives have uneven character in point of transition. This classification may be expanded on phase transitions of more high order. For example, transition from liquid in superfluidity state is third-order phase transition.

Further expansion of thermodynamic theory of phase transformations is the L. Landau phenomenological theory of second-order phase transitions [1, 7]. He introduced the order parameter. Behavior of these parameters in the point of transition allows modeled proper phase transformations more detail [7].

An order parameter is fundamental macroscopic variable [7]. It may be have various physical nature (density, magnetization, polarization, concentration a.o.).

In general case structural phase transitions may be created of condensation various phonon modes, including nonpolar. In this case the condensation of soft mode is happened in one of symmetric point of Brillouin zone. These points are famous as Lifshitz points [8]. In the results of its phase transitions the structures with period, which is divisible to period of Bravais lattice; may be happened. Periods of structure of these low symmetric phases are divisible to periods of initial Bravais lattice with divisible $n = 1, 2, 3$. Maximal increasing of volume of elementary cell is divisible 32.

Possibility of the condensation of soft mode in some point of Brillouin zone is determined of peculiarities of phonon spectrum the concrete system, more precision, the place of minimum in disperse curve of soft mode. The existence of this minimum in some symmetrical point of Brillouin zone isn't a consequence symmetrical conditions, it depend from the peculiarities of the interatomic interaction of concrete crystal. Therefore may be happen situation, when minimum of soft mode will not correspond to symmetrical point of Brillouin zone. The condensation of this phonon is caused to the creation a structure with period, which is aliquant (incommensurate) to a period of initial crystal structure. For the phase transitions, which is corresponded to stars of Lifshitz type, module of wave vector can change continuously without a change of structure. Therefore, period of this structure is arbitrary (divisible to irrational number) relatively to a period of a lattice initial symmetric phase. Crystal phases, which are characterized of Lifshitz type vectors, are called incommensurate phases [8 – 11]. These phases may be created in the result structural, magnetic, mesomorphic and other types of phase transition.

Incommensurate phases have various natures. But R.A.Cowley and A.D.Bruce [9 – 11] united its in two types. Type I is determined hypothetical phase transition from initial to incommensurate phase with a change of translational symmetry. Incommensurate phases of type II are determined the class of incommensurate materials in which initial and incommensurate phases are equitranslational.

This classification is included classic crystal phases (230 space Fedorov groups) [2, 4] and another more low-indexes symmetry, which are represented another structures.

As statistical expansion of thermodynamic theory of phase transitions may be represented Lee-Yang theory [6].

Thermodynamic theory of phase transitions isn't including the temporal characteristics of proper processes. Roughly speaking it is the macroscopic averaging of microscopic processes.

The phase transition theory, which is allow to observe phase transition between phases of various dimensions, was called theory topological phase transitions. So, this theory allows observing transition from three-dimensional to two-dimensional phase [12]. Transitions between various networks of chalcogenide glasses are classified as structural-topological phase transitions too [13].

But we have many other processes, which are explained phase transformations in matter after influence some external actions. It may be irreversible chemical reactions, including processes of combustion and explosion [14]. Some these processes aren't average but they characterize phase transformations or creation new phases. Difference from thermodynamic case is the causality of these transformations. In Erenfest case it is the heating, which is caused the increasing of atomic oscillations in matter. In other cases, these causes may be having other nature: chemical elements, various types of irradiation and other.

We can remark fact that theories of combustion and explosion are based on enthalpy, theory of elastic bodies on Helmholtz potential (free energy) [14]. But first and second theories explain the irreversible processes and third theory – non-equilibrium processes. These processes may be represented as phase transformations too.

Chemical reactions, including ionization, may be represented as phase transformations. But chemical reactions are modeled with help of methods of chemical kinetics, including photochemical, thermochemical and self-oscillation. But kinetic processes have dynamic nature and for large numbers of processes the procedure of thermodynamic averaging isn't necessary.

More complex processes of phase transformations may be modeled as cascade processes [4, 15]. Conditions of arising new phases can be various and it may have various natures. Causes of formation proper "members" of cascade processes may have various directions: from low symmetry to more high symmetry and inversely from high symmetry to more low symmetry. The example of first process is the laser annealing of semiconductors and example of second process is the laser implantation of solid. These processes may compete. So, for the case of light scattering on stables centers photochemical and thermochemical processes have various directions. But for the case of light scattering on unstables centers these processes may be have one direction [4]. Self-oscillation processes may be received with help of using two regimes of irradiation: straight process irradiation in self-absorption range and back irradiation in "damage" absorption range, which is received in the time of straight process.

For the modeling phase transformations may be used methods of synergetic [1, 16] and catastrophe theory [16]. Roughly speaking each catastrophe is phase transition [16] or chemical reaction [4, 16].

Rough bond between thermodynamic and kinetic concepts of phase transformations may be represented with help de Broglie formula, which is used in thermodynamics of point [17]

$$\frac{S_a}{\hbar} = \frac{S_e}{k_B}, \quad (1)$$

where S_a – action, S_e – entropy, $\hbar$ – Planck's constant, k_B – Boltsman constant.

Formula (1) allows subscribing mutual transitions from quantum (kinetic) to statistical (thermodynamic) processes. It may be represented as foundation of bond quantum (kinetic) and statistical physics (thermodynamics) [17].

III. EXPERIMENTAL DATA

Now we represent of some experimental data of RO, which will model. We select laser-induced surface phase transformations, which are caused the mechanisms of self-absorption; and volume phase transformations, which are connected with intrinsic mechanisms of light absorption. It allows observing basic peculiarities of proper physical processes and methods of its modeling.

First experimental data of irreversible interaction the laser radiation and semiconductors were received by M. Birnbaum in 1965 [18]. He observed the surface interferograms after pulse Ruby-laser irradiation of germanium, silicon, indium antimonite a.o. [18]. These results are beginning of researches of surface laser-induced phase transformations. The volume laser-induced phase transformations systematically were begun by B. S. Sharma [19]. He observed laser-induced damages in glasses after pulse Ruby laser irradiation..

Later these results were developed to interference laser annealing of semiconductors [4]. But this fact is corresponded to the structural changes of laser-irradiated pure matter and matter with impurity and damages. Impurities and damages in the irradiated material have little influence on the formation of the surface interferogramms [4]. Nanostructures formed by crest of interferograms. Its formation is depended from parameters of irradiation. Therefore these phenomena have more deep nature as laser annealing of ion-implanted materials [4].

Surfaces nanostructures were received after irradiation of SiO_2/Si structure by second harmonic Nd:YAG laser at density of power I=2.0 MW/cm^2, pulse duration 10 ns, wavelength 532 nm and frequency of repetition 12,5 Hz (Fig. 1) [20].

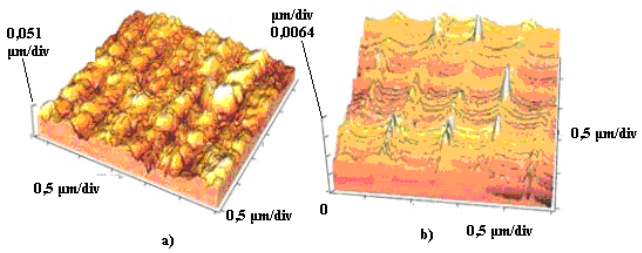

Fig. 1: AFM 3D images of: (a) SiO_2 surface after irradiation of SiO_2/Si structure by second harmonic Nd:YAG laser at I=2.0 MW/cm^2 and (b) Si surface after subsequent removing of SiO_2 by HF acid [20].

More detail research of creation the surface laser-induced structures are represented by A. Medvids in [20]. Samples of *Ge* {111} and *Ge* {001} i-type single crystals are used in experiment. Nd:YAG laser (wavelength 1,064 μm, duration of pulse 15 *ns*, pulse rate 12,5 *Hz*, power P=1 *MW*) was used for the irradiation.
The AFM picture of *Ge* surface after *Nd* laser irradiation is represented in Fig. 2 [20].

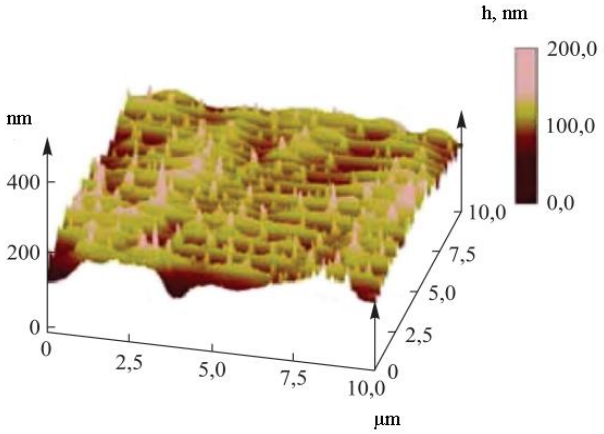

Fig. 2: Three-dimensional AFM image of nanostructures after Nd:YAG laser irradiation with density of power 28 MW/cm^2 on Ge surface [20].

More large columns (height 20 μm, diameter 2 – 3 μm) were received after irradiation of pulse series the nanosecond eximer KrF-laser (wavelength 248 *nm*, pulse duration 25 *ns*) (Fig. 3). This figure illustrates the high aspect ratio silicon micro-columns that were formed in air after 1000 laser shots at an energy density, E_d , between 2.7 and 3.3 J/cm^2. The columns are ~20 μm long and ~2~3 μm in diameter. Moreover, surface-height profilometry performed using a Dektak II profiler revealed that most of the length of the microcolumns, 10 – 15 μm, protrudes above the original Si surface [21].

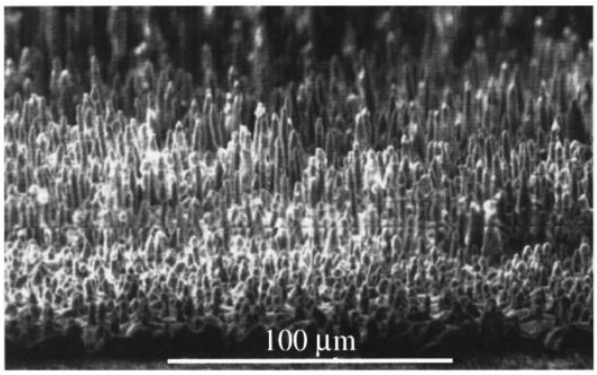

Fig. 3: SEM images of silicium nanocolumns after 1000 laser shots in air at $E_d = 3 J/cm^2$ [21].

The microcolumn morphology changes if the atmosphere is changed during laser irradiation. Fig. 4a shows several columns in a specimen that was first irradiated with 600 pulses in air and 1200 pulses in $N_2/5\%O_2$ [21, 22].

The importance of the gas environment was emphasized, when a plasma etchant, SF_6, was used as the ambient gas during laser irradiation of silicon [21, 22]. In SF_6 extremely long structures are produced that look at first like walls surrounding very deep central holes (see Fig.4b) [21, 22].

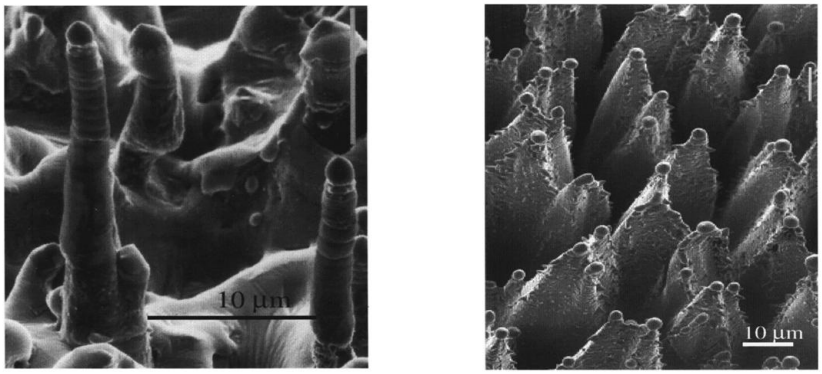

Fig. 4: a) SEM image showing a change in Si microcolumn morphology controlled by the ambient gas composition at E_d = 2.7 J/cm^2. The arrows indicate the height achieved after 600 laser pulses in air (N_2 – 18% O_2); the remainder of the columns was grown by 1200 laser pulses in N_2 – 5% O_2; b) Walled Si structure produced by 2040 laser pulses at E_d =1.5 J/cm^2 in 1 atm of SF_6 [21, 22].

Ordered laser-induced nanostructures, which were created on surface of Si after laser irradiation (λ = 0,8 μm, τ_i = 100 fs, number of pulses 200) through lay of water, are represented on Fig. 5. Three types of micro and nanostructures are generated [4, 23, 24]. Nanostructures have typical spatial scale d_1=600 *nm* and d_2=120 *nm*, here lattice vector oriented $\vec{g} \parallel \vec{E}$. It is corresponded to interference between surface polariton-plasmon (SPP) and TM electromagnetic wave. Structures with period d_1 are generated for interference of falling wave with SPP wave, which arise on the border water – free electrons of silicon. Structures with period d_2 are generated for mutual interference of two SPP, which were propagated in mutually inverse directions along border silicon – plasmic layer. Structures with period 120 *nm* aren't depended from nature of liquid, which was contacted with silicon [24]. It is experimental fact.

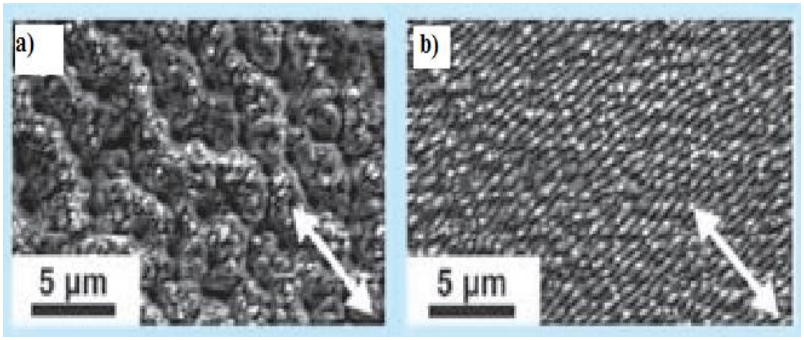

Fig. 5: Ordered structures, which were generated on surface of silicon after laser irradiation through lay of water, (arrow in lower angle show the direction of polarization of laser radiation); duration of pulse 100 *fs*, wavelength – 800 *nm*, number of pulses 200, density of energy the irradiation a) 25 kJ/m^2, b) 5 kJ/m^2 [23].

Laser-induced silicon nanostructures (λ = 0,8 μm, τ_i = 100 *fs*, number of pulses 200) with d_3=90 *nm*, which was generated after irradiation structures of changing polarization with d_2=120 *nm*, when orientation of vector $\vec{E}$ was changed on 90° relatively to initial action. Power of laser irradiation was less in two times as for initial structure. Generated periodical structures (Fig. 6d are nanocolumns with height to 400 *nm* with spatial period 90 nm and orientation wave vector $\vec{g} \parallel \vec{E}$ [23, 24]. Where ğ is beam propagation direction.

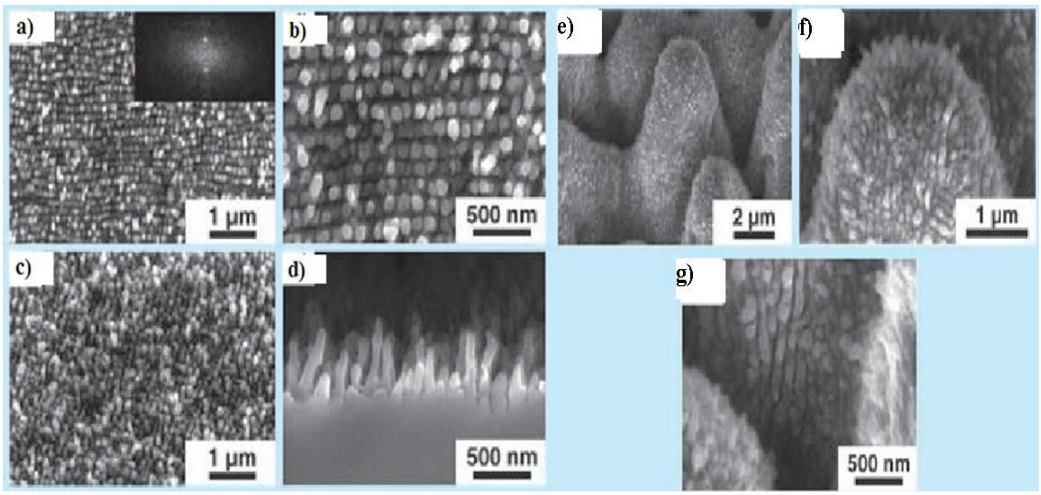

Fig. 6: Nanocolumns, which are generated after irradiation structures of silicon with d_2=120 nm, (wavelength of irradiation 800 nm, number of pulses – 200, density of energy of irradiation 0,5 kJ/m^2): a) and b) turn of polarization on 90°, c) turn of polarization on 45°, d) cross chip of nanocolumns. On insertion to Fig. 7a – Fourier-picture of structures [13]; e) – f) Surface silicon nanocolumns of little scale, which have orthogonal orientation to a crests of nanorelief of large scale [23].

Generation of periodical nanostructures along crests (d=90 nm) is caused of interference the falling radiation with surface polaritons, which are exited along crest of relief (d~120 *nm*), and with mutual interference of surface polariton-plasmons [24]. A crest of relief, which considered in contact with the substrate, was selected as initial half-cylinder. Formed in this case inoculating regular relief d~90 nm is basis for further growth of nanocolumns. Since typical radius of half-cylinder $r << \lambda$, therefore dispersion relation for surface polariton-plasmon in cylindrical geometry is changed from dispersion relation in plane geometry of phase separation. It cause to formation nanostructures with less period as for plane case [24].

For case of elliptic polarization and falling angle to surface from 0 to 20° basic nanostructures are created: 1) surface nanostructures with period ~200 *nm* and 2) these structures with period 70–100 *nm* are generated on crest of structure 1, but its orientation $\vec{g} \perp \vec{E}$ [24].

Basic difference between nanosecond (Fig. 1, Fig. 3, Fig. 4) and femtosecond regimes of creation of surface silicon nanostructures (Fig. 5, Fig. 6) is the its sizes: 15-20 nm for nanosecond regime of irradiation (nanohills) for Neodimium laser (Fig. 1), 20 – 50 μm for eximer laser (Fig. 3 and Fig. 4) and 400-450 nm for femtosecond regime of irradiation (Fig. 5, Fig. 6). These data are proved electromagnetic mechanisms of creation surface nanostructures (surplus of negative charge is caused the electromagnetic swelling of surface) [4, 25, 26]. Heat processes are caused the decrease of sizes, including height of surface nanostructures. But we have nanosecond laser-generated silicon microstructures (Fig. 3, Fig. 4) and 200 nm germanium microstructures (Fig. 2), which are shown an influence of intensity and mechanisms of light absorption and number of pulses on the generation surface structures.

For the modeling processes of Fig. 2 – Fig. 6 we must develop electromagnetic concept of RO. This concept allows including in parametric optical processes back side of "medal": resulting trace of interaction light and matter in matter [2 – 4, 25, 26].

An influence of pulses number on the processes of formation of laser-induced periodic nanostructures on titanium plate is observed in [9]. Sapphire laser system was used for the irradiation. It had next parameters: wavelength 800 *nm*, repetition rate 1 *kHz*, pulse length 100 *fs*, beam diameter 4 *mm* and density of energy of irradiation 0,25; 0,75 and 1,5 *J/cm*^{2}. Interference structures are generated for the irradiation with energy density 0,25 J/cm^2 [27]. Evolution of creation the laser-induced surface structures are represented in Fig. 7.

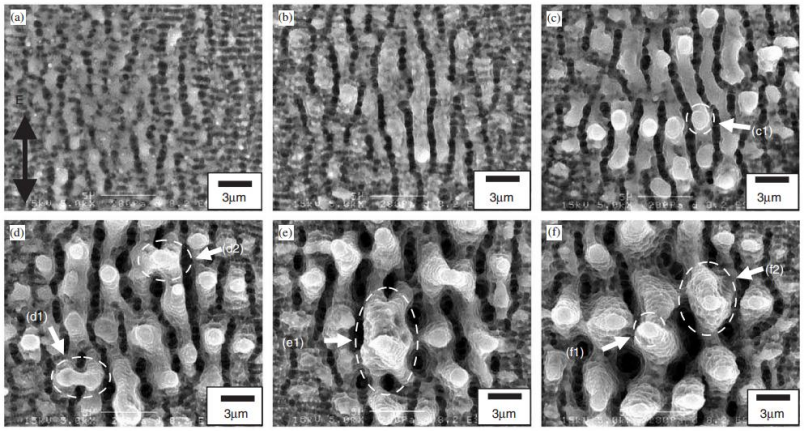

Fig. 7: Microstructures produced on the titanium plate at the laser fluence of 0.75 J/cm^2 for (a) 10, (b) 25, (c) 50, (d) 70, (e) 90 and (f) 110 pulses [27].

The period of the parallel periodic microstructures as a function of the number of laser pulses is shown in Fig. 8a [27]. As shown in Fig. 8a, the period was gradually increased in the range of 10–70 pulses and increased in the range of 70–110 pulses as the number of pulse increased.

Distance between the microdots along the hill of periodic microstructures as a function of the number of laser pulses is shown in Fig. 8b [27]. As Fig. 8b shows, the distance was increased in the range of 50–110 pulses. But these distances are correlated with height and width of inetrferogram bands (Fig. 7).

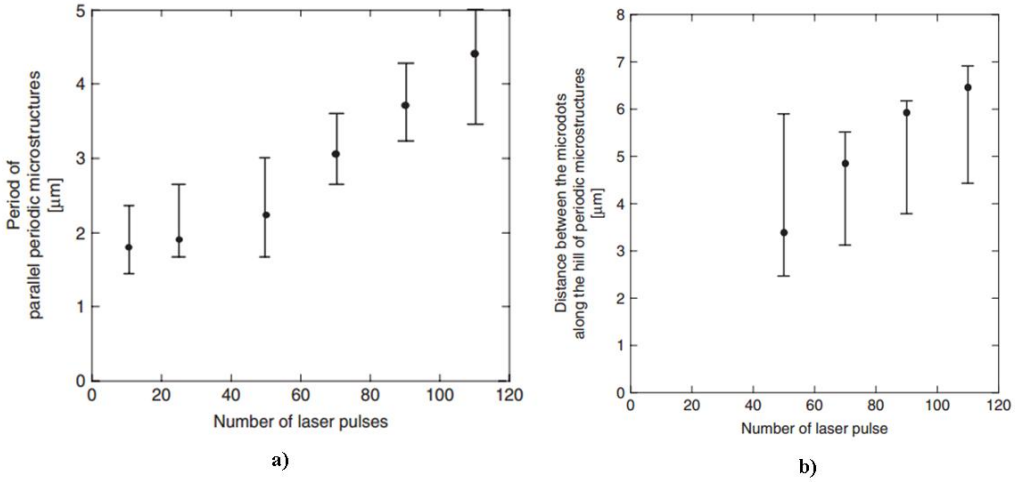

Fig. 8: a) Period of parallel periodic microstructures as a function of number of laser pulses; b) Distance between the microdots along the hill of periodic microstructures as a function of the number of laser pulses [27].

Basic peculiuarities of the creation the volumr laser-induced phase transformations are represented in Fig. 9 [28, 29].

In [28, 29] for minituarization of receiving structures of crystals 4H-SiC were irradiated by pulses of femtosecond laser (duration of pulses 130 *fs*, wavelength 800 *nm*, frequency of pulses 1 *kHz*, density of energy 200-300 *nJ*/pulse) with help microscope.

Conditions of irradiation are represented in Fig. 9 ((a), (b)) [28]. Femtosecond laser pulses were irradiated along the lines inside 4H-SiC single crystals at a depth of 30 μm by moving the sample at a scan speed of 10 $\mu m/s$. The laser beam was irradiated at a right angle to the (0001) surface of the crystal. The irradiated lines were almost parallel to the $\left[1\bar{1}00\right]$ direction. A schematic illustration of the laser-irradiated pattern is shown in Fig. 9 (a). The distance between neighboring lines was 20 μm.

Bright-field TEM (transmission electron microscopy) image of the cross section of a line written with a pulse energy of 300 *nJ*/pulse is shown on Fig. 9 ((c) – (e)) [29].

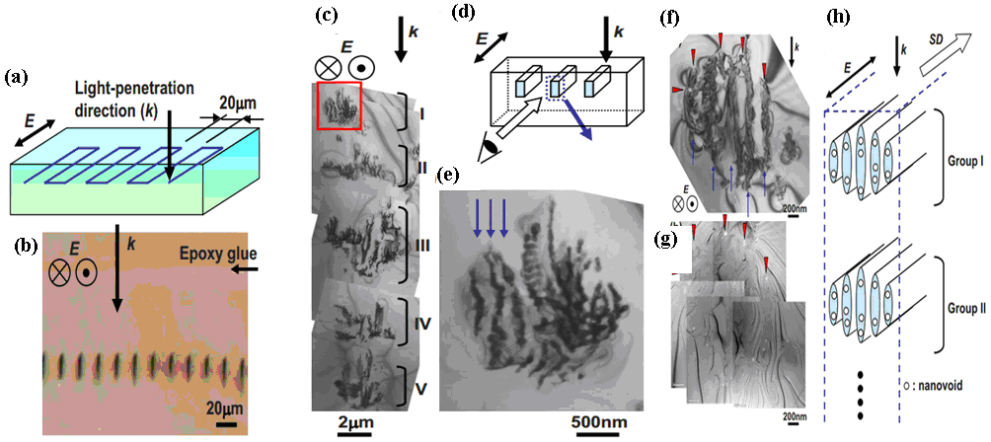

Fig. 9: (a) Schematic illustration of the laser irradiated pattern. The light propagation direction (k) and electric field (E) are shown. (b) Optical micrograph of the mechanically thinned sample to show cross sections of laser-irradiated lines (200 nJ/pulse). (c) Bright-field TEM image of the cross section of a line written with pulse energy of 300 nJ/pulse. (d) Schematic illustration of a geometric relationship between the irradiated line and the cross-sectional micrograph. (e) Magnified image of a rectangular area in (a). Laser-modified layers with a spacing of 150 nm are indicated by arrows. (f) Bright-field TEM image of a portion of the cross section of a line written with a pulse energy of 200 nJ/pulse. (g) Zero-loss image of a same area as in (f) with nanovoids appearing as bright areas. Correspondence with (f) is found by noting the arrowheads in both micrographs. (h) Schematic illustrations of the microstructure of a laser modified line. Light-propagation direction (k), electric field (E), and scan direction (SD) are shown. Only two groups (groups I and II) of the laser-modified microstructure are drawn [28, 29].

In contrast to the formation of surface periodical structures three-dimensional periodic structures were obtained in this case. Sectional area of these structures was ~ 22 *μm*, the depth of ~ 50 *μm*. As seen from Fig. 9(c) we have five stages disordered regions, which are located at a distance from 2 to 4 *μm* apart vertically [22]. Branches themselves in this case have a thickness from 150 to 300 *nm*. In this case there are lines in the irradiated nanocavity spherical diameter of from 10 *nm* to 20 *nm*. In this case irradiated structures have crystallographic symmetry of the initial structure.

More detail information about processes, which are generated in first two stages, represents in Fig. 9 ((f) – (h)) [29].

IV. Modeling And Discussions

The methods of modeling the phase transformations in Relaxed Optics must be based on the concept of saturation of excitation, which is basic for laser physics and theory of phase transitions [2 – 4]. H. Haken used this analogy for the modeling Nonlinear Optical phenomena as nonequilibrium phase transitions [1]. But classic Nonlinear Optical processes is processes of nonequilibrium impurities light scattering in solid with impurity concentration $10^{15} – 10^{16}$ cm^{-3}. In this case we have radiated relaxation (effects of Linear and Nonlinear Optics) [2]. For case of self-absorption we can have radiated and unradiated relaxation. The last is cause of Relaxed Optical Processes [4]. Therefore we accented attention on this moment for the explanation experimental data of Fig. 1 – Fig. 8.

Therefore we must estimate all possible mechanisms of relaxation: kinetic and dynamical; and possible mechanisms of excitation: hierarchical photo-ionization. In this case we must include respective chain of relaxation times [4, 15]. It is necessity for the more full representation and modeling real and possible physical processes for the respective regimes of interaction.

Thus this representation of the modeling dangling bonds, which are created with help laser irradiation, is very effective method. It allows including in consideration effects of equilibrium, nonequilibrium and irreversible relaxations [4].

Now we show the using of cascade model for the explanation experimental data of laser-induced phase transformations in silicon, germanium, carbon and titanium. It was called as case the structural phases.

The question about the influence of saturation of excitation on effects of RO may be represented as process of transitions between stable and metastable phases too. Now we'll estimate the influence of parameters of irradiation (including spectral) on irreversible changes and transformations in *Si* and *Ge*. Spectral dependences of absorbance of various structural modification of Si are represented in [30]. Now we'll be

estimated intensities of eximer, Ruby and Neodymium laser irradiation (wavelengths of irradiation are 0,248 μm, 0,69 μm and 1,06 μm properly of silicon and germanium, which are necessary for the creation of proper irreversible changes in irradiated semiconductor. As shown in [30], absorbance of the Neodimium laser radiation in silicon is equaled 100 cm^{-1}, second harmonic of Neodimium laser – 10^4 cm^{-1}, eximer laser – 10^6 cm^{-1}.

Crystal semiconductors Si and Ge have, basically, the structure of diamond. Volume atomic density of elementary lattices may estimate according to formula [1]

$$N_a = \frac{\rho N_A}{A}, \qquad (2)$$

where ρ – density of semiconductor, N_A – Avogadro number, A – a weight of one gram-atom. For *Si* $N_{aSi} = 5 \cdot 10^{22}$ *cì* $^{-3}$ and for *Ge* $N_{aGe} = 4,4 \cdot 10^{22}$ *cì* $^{-3}$.

But *Si* and *Ge* may be crystallized in lattices with hexagonal, cubic, trigonal and monoclinic symmetry. Phase diagram of Si as function of coordination number is represented on Fig. 10 [31].

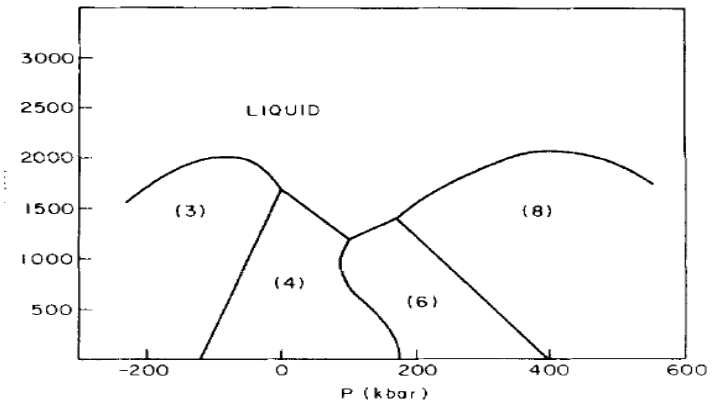

Fig. 10: A schematic phase diagram for *Si*(CN). The coordination numbers (CN) of the various phases are indicated. The diagram is based on common features of the phase diagrams of column IV elements as described by the references cited in Pistorius's review (Ref. 8 in [31]). Starting from a high tempera-ture >3□10^3K and subject to a constraint of average density $\langle \rho \rangle = \rho(4)$, a hot micronucleus will tend to bifurcate into the most stable phases (highest T_m) which straddle *Si*(4) in density. These are *Si*(3) and *Si*(8), as indicated by the diagram [31].

Coordination number (CN) 8 is corresponded of diamond lattice, CN 6 – hexagonal lattice, CN 4 and CN 3 – other two lattices. It should be noted that melting temperatures of these phases are various. Volume density of CN is equaled CN·N_a. For diamond symmetry of lattice this value is $8N_a$.

Roughly speaking, transition from one phase to another for regime of saturation of excitation may be modeled as one-time breakage of proper numbers of chemical bonds, which are corresponded to the difference of CN of proper phases. For example, two bonds breakage is caused the phase transition from diamond to hexagonal structure. One bond breakage in the regime of saturation is caused to generation of laser radiation.

Results of calculation of volume densities of energy, which are necessary for breakage of proper number of bonds in regime of saturation of excitation, are represented in Table 1. It conceded that energies of all chemical bonds for elementary lattice are equivalent (*Si* and *Ge* are pure homeopolar semiconductors) [4]. For silicon energy of covalent bonds *Si-Si* are equaled 1,2–1,8 *eV*; for germanium energy of covalent bonds *Ge–Ge* are equaled 0,9–1,6 *eV*. Minimal values of these energies are corresponded of Pauling estimations. These values are corresponded the energy on one CN: according to radiation physics of status solid Zeits energy of creation one radiation defect is equal 12,7 *eV* for diamond lattice [32]

.

Table 1: Volume density of energy I_{vi} (10^3 *J*/*cm*^{3}), which is necessary for the breakage of proper number of chemical bonds in the regime of saturation of excitation in *Si* and *Ge* [25, 26].

Semiconductor	I_{v1}	I_{v2}	I_{v4}	I_{v5}
Si	12,8 – 14,4	25,6 – 28,8	51,2 – 57,6	63 – 72
Ge	6,3 – 8,4	12,6 – 16,8	25,2 – 33,6	31,5 – 42

Surface density of energy on proper numbers of CN for proper lasers irradiation may receive after division of results of Table 1 on proper absorbance. This procedure allows to transit from bulk to surface density

of energy, which is necessary for the receiving of proper phenomena. Results of these calculations are represented in Table 6.

It should be noted that real regimes of irradiation must be more (process of light reflection wasn't included in our estimations). In addition we aren't include the relaxation (time) processes for the scattering of light on stable centers (self-absorption in crystals) as for *InSb* and *InAs* [15].

Table 2. Surface density of energy I_{si} (J/cm^2), which are necessary for the breakage of proper numbers of chemical bonds in *Si* and *Ge* crystals after proper lasers irradiation in regime of saturation the excitation [25, 26]

Semiconductor and wavelength of irradiation	I_{s1}	I_{s2}	I_{s4}	I_{s5}
Si, 1,06 μm	128 – 144	256 – 288	512 – 576	630 – 720
Si, 0,80 μm	12,8 – 14,4	25,6 – 28,8	51,2 – 57,6	63,0 – 72,0
Si, 0,53 μm	1,28 – 1,44	2,56 – 2,88	5,12 – 5,76	6,3 – 7,2
Si, 0,248 μm	0,0128 – 0,0144	0,0256 – 0,0288	0,0512 – 0,0576	0,063 – 0,072
Ge, 1,06 μm	0,63 – 0,84	1,26 – 1,68	2,52 – 3,36	3,15 – 4,2
Ge, 0,53 μm	0,32 – 0,42	0,63 – 0,84	1, 26 – 1,68	1,58 – 2,1

Remark to Table 2: absorbencies α_i of *Si* (Neodimium laser) – 100 cm^{-1}; *Si* (wavelength 0,8 μm) –$\circledcirc 10^4$ cm^{-1}; *Si* (second harmonic of Neodimium laser) –$\circledcirc 10^4$ cm^{-1}; *Si* (eximer laser) – $\circledcirc 10^6$ cm^{-1}. *Ge* (Neodimium laser) –$\circledcirc 10^4$ cm^{-1}; *Ge* (second harmonic of Neodimium laser) – $2\circledcirc 10^4$ cm^{-1}.

The values of Table 2 are corresponded to the light absorption on the length absorption $l_{abi} = \frac{1}{\alpha_i}$. But absorbencies are changed in the process of irradiation (blooming process). The irradiated surface is changed with increasing of number of pulses the laser irradiation.

Now we estimate the experimental regimes of irradiation and make comparative analysis with data of Table 1 and Table 2.

Mechanisms of creation other laser-induced nanostructures may be explained on the basis cascade model of step-by-step excitation of corresponding type and number of chemical bonds in the regime of saturation of excitation. According to this model decrease of symmetry of irradiated matter is occurred with increase of intensity of irradiation (*Nd* laser irradiation of silicon, germanium and carbon) [4, 25, 26].

Representation of experimental data of Fig. 4 in terms of Tables 1 and 2 we are realized in next way. The energy, which is necessary for creation one microcolumns with hexagonal or trigonal symmetry is equaled $E_{mci} = E_{vi}V_{mc}$, where V_{mc} – volume of microcolumn. For the cylinder approximations with average radius of cylinder 5 μm, maximal radius of cylinder 10 μm and height of cylinder 50 μm we have $E_{mchex} = E_{v2}V_{mc} = 10^{-4}\,J$ $E_{mctrig} = E_{v4}V_{mc} = 2\cdot 10^{-4}\,J$. Surface density of energy may be received in next way: we must multiply last results on the density of microcolumns, which is equaled $0{,}86 \big/ \pi r_{mc\max}^2 = 2{,}7\cdot 10^5\, mc \big/ cm^2$. Therefore $E_{mchexs} = 27\, J \big/ cm^2$ and $E_{mctrigs} = 54\, J \big/ cm^2$. But these results are corresponded to effective length of absorption 50 μm. Let effective length of absorption of our multipulse regime of irradiation is equaled 0,05 μm. Then we have $E_{mchexsr} = 0{,}027\, J \big/ cm^2$ and $E_{mctrigsr} = 0{,}054\, J \big/ cm^2$.

We can estimate the volume density of energy of irradiation for Fig. 4b. In this case we have effect of increasing blooming, therefore average absorbance is equaled $5\cdot 10^4$ cm^{-1}, therefore effective volume density of energy may be determined as $\frac{2{,}7\cdot 5\cdot 10^4}{2{,}5} = 54\, kJ\cdot cm^{-3}$. This value is corresponded the break of fourth bonds and creation minimum two phases according to Table 2: hexagonal (macrocolumns of Fig. 5b) and trigonal (microcolumns of Fig. 5b). These estimations are very rough but it allows explaining basic peculiarity of creation anomalous large surface laser-induced structures. We include reflectance, which is equaled 0,6. Therefore we have almost maximal use the irradiation energy to phase transformations in irradiated matter.

The creation of hexagonal nanostructures on *Ge* surface (Fig. 2) has other nature. It must be multiphotonic processes, which is increased the absorbance. We can estimate this process according to Table 2. The effective coefficient of absorption may be determined as $E_{isest} = E_{vi}\cdot d$, where d – high of nanocolumn/. After substitution of proper values we have $E_{2sestGe} = 0{,}0252\, J \big/ cm^2$ and $E_{4sestGe} = 0{,}0504\, J \big/ cm^2$, real value is equaled

0,36 J/cm^2 . Therefore the effective using of laser irradiation is equaled 0,056 – 0,112. Analogous estimations of femtosecond pulse irradiated nanocolumns (Fig. 7e) are next $E_{2sestSi} = 1{,}152\ J/cm^2$ and $E_{4sestSi} = 2{,}304\ J/cm^2$, effective using is equaled 0,01 – 0,05.

Height of surface nanostructures for the nanosecond regime of irradiation is maximal (200 *nm*, Fig. 2) for the germanium [20] for small number of pulses and for silicon (20 – 50 μm, Fig. 3, Fig. 4) for large number of pulses [21, 22]. For the silicon (Fig. 1) height of laser-generated surface nanostructures is change from 10 *nm* to 20 *nm* [20]. This difference can be explained in next way. Index of light absorption with wavelength 532 *nm* of *Ge* crystal with diamond symmetry is more as silicon with this symmetry for the nanosecond irradiation. But surface part of irradiated germanium is transited to hexagonal phase. It is experimental data. Other result given's phase transitions. The hexagonal lattice of germanium has greater size as diamond modification. Therefore hexagonal nanostructures are greater and more stable as polycrystalline or metallic nanohills.

But in [20] the explanation of creation laser-induced hexagonal phase on germanium surface is based on the Benar phenomenon: generation of hexagonal phases in heated liquid on roaster. This effect is observed for few liquids. Chandrasekar theory is described this process as thermal-diffusive processes [1, 33]. In this case we have transition from more low volume symmetry to more high surface symmetry. Chandrasekar created the hydromagnetic theory of creation sunspots [33].

For laser-induced creation volume hexagonal structures on *Ge* we have inverse transition: from high volume symmetry (diamond modification) to more volume low symmetry (hexagonal symmetry) [20].

The influence of pulse numbers on generated the surface interferograms on titanium was received in [27] (Fig. 9). For explanation these results may be used the cascade model of saturation the excitation. Irradiated titanium has two phases: α-phase (hexagonal) and β-phase (body-centered cubic lattice). Temperature of phase transition α → β is equaled 882,5°C [34]. Hexagonal structure has more large electronegativity, therefore the interference maximum of Fig. 9 must be have α-symmetry. Increasing of number pulses is caused of saturation the interference band and generation nano and microstructures.

The mechanisms of light absorption are influenced on the relaxation time of excitation. Proper phenomenological chain of relaxation times is represented in [4, 15]. The number of disrupt chemical bonds or CN may be determined with help next formula

$$n = 2\ln\frac{h\nu}{E_a}. \quad (3)$$

Where E_a – the energy of ionization (breakage) of proper bond.

More pure ionizing results were received for the irradiation silicon by femtosecond laser pulses in multipulse regime [13]. One quantum of eximer laser radiation may be ionized 3,5 chemical bonds according to formula (4). Therefore multipulse regime of the irradiation is caused the generation silicon structures with hexagonal and trigonal symmetry. Density of energy 2,7 J/cm^2 (Fig.5) and 1,5 J/cm^2 (Fig. 6) certificated this hypothesis according to Table 2. First regime (Fig. 5) allows receiving more thin and high structures with more low symmetry, which is stipulated more high intensity of irradiation. Second regime (Fig. 6) may be results of generation the structures with more low symmetry (no cubic). Atmosphere of irradiation must be has neglected influence on finishing picture. This conclusion is certificated by experimental data of Fig. 4 – Fig. 6.

For light absorption on unstable centers (amorphous semiconductors) time characteristics haven't large observable influence on formation of irreversible changes in semiconductors. Here integral dose of irradiation has general meaning; therefore in this case photochemical ionizing processes give basic contribution and processes of radiated relaxation are neglected.

With including of light reflection data of Table 2 must be increased on 20-30 percents for regimes of irradiation the Nedimium laser (both regimes) and 250 percents for eximer laser irradiation (reflectance of eximer laser radiation is equaled 60 percents).

In addition we must remember that Ruby laser radiation for crystalline silicon has absorbance on order less as for amorphous, therefore for short regimes of irradiation the processes of bonds breakage may give more influence as for case of Nd-laser irradiation. Polycrystalline layer may include various crystalline phases. We can select condition of irradiation with creation on surface of silicon the nanostructures with various its fourth crystallographic modifications.

The role of irradiated atmosphere on formation of laser-induced surface nanostructures is shown in Fig. 1, Fig. 4 – Fig. 8. An oxidation processes are smooth out the surface (Fig. 1 and Fig. 5). The decreasing of oxygen concentration is caused the more intensive growth of microcolumns (Fig. 3, Fig. 4) and nanocolumns (Fig. 1, Fig. 2, Fig. 5 – Fig. 8).

The cascade model may be used for the explanation of experimental data of Fig. 1 – Fig. 8. Titanium has two phases: hexagonal and body-centered cubic. But after heating the titanium to 882,5°C it has only cubic

phase [34]. According to cascade model peaks of proper surface columns must have hexagonal symmetry, but its generation is attended with oxidation processes. Therefore the intensities of creation the surface structures are various for two groups of pulses: for second group (70 – 110 pulses) is more intensive process as for first group of pulse (10 – 50 pulses). Among these regimes of irradiation may be receive the doubling of period of interference pattern (Fig. 9).

This method was used for the explanation of the experimental data about laser-induced transformations in various allotropic phases of carbon, included diamond, graphite, fullerenes and other [4] too.

For more precisius modeling we must include the chain of relaxation times analogous as in case of indium atimonite [15]. This procedure allows selected the proper nonlinear and relaxed optical processes [2, 35].

Roughly speaking cascade model may be represented as "kinetic" addition to classical theory of phase transitions. The chain of coordination numbers is the "kinetic" discrete order parameter.

Other picture we have for laser-induced volume phase transformations in SiC (Fig. 9). Explanation of the experimental data, which are shown in Fig. 9 is based on nanoplasmic model [27]. The emergence nanovoids explained on the basis of the explosive mechanism. However, the same result can be explained by the formation of vacancy clusters, especially those sizes of nanovoids same are equivalence to sizes of nanoclusters. Nanovoids, as a rule, are formed between the most modified regions, i.e. in these areas there are sinks of vacancies [32], which form the nanovoids or vacancies clasters.

Nanovoids may be represented as results of the laser-induced laser-induce break-down and creation of cavitation bubbles [36 – 39] too. The light pressure may be determined with help of next formula [19]

$$p_0 = \frac{E_{ir}}{\tau_i c S}, \quad (4)$$

where E – energy of irradiation, τ_i – pulse duration, S – area of irradiation zone, c – speed of light. For circle symmetry

$$S = \pi r^2, \quad (5)$$

where r – radius of laser spot.

For the estimations of maximal radius of nanovoids we must use modified Rayleygh formula [37]

$$R_{\max} \approx \frac{T_c}{0{,}915}\sqrt{\frac{p_0}{\rho_0}}, \quad (6)$$

where T_c – the time of creation the nanovoid (bubble), ρ_0 – the density of irradiated matter.

Time T_c may be determined as

$$T_c \approx \frac{d_c}{\vartheta_s}, \quad (7)$$

where d_c – characterized size of nanovoid (cavitation bubble), ϑ_s – speed of sound. For the spherical symmetry $d_c = 2R,$ where R is radius of nanovoid.

The speed of sound may be determined as [14, 40, 41]

$$\vartheta_s = \sqrt{\frac{E}{\rho_o}}, \quad (8)$$

where E – Young module [14].

The finished formula for determination $R_{\max}$ has next form

$$R_{\max} \approx \frac{2R}{0{,}915r}\sqrt{\frac{E_{ir}}{\pi\tau_i c E}}. \quad (9)$$

If we substitute r = 250 *nm*, R = 10 *nm*, E=600 *GPa* [40, 41], E_{ir}=130 *nJ*, τ_i = 130 *ps*, c=3·10^8 *m/s* in (9), than have $R_{\max}$=11 *nm*.

The speed of shock waves for femtosecond regime of irradiation is less as speed of sound. But we have two speeds of sound in elastic body: longitudinal ϑ_{ls} and transversal ϑ_{ts} [14]. Its values are determined with next formulas

$$\vartheta_{ls} = \sqrt{\frac{E(1-\nu)}{\rho_o(1+\nu)(1-2\nu)}}, \text{ and } \vartheta_{ts} = \sqrt{\frac{E}{2\rho_o(1+\nu)}}, \quad (9)$$

where v – Poisson's ratio [14]. The ratio between of these two speeds is equaled

$$\alpha = \frac{\vartheta_{ts}}{\vartheta_{ls}} = \sqrt{\frac{(1-2\nu)}{2(1-\nu)}}. \quad (10)$$

But this ratio must be true for shock waves too. Therefore for silicon carbide for v = 0,45 [40, 41] α = 0,33. Roughly speaking last ratio is determined the step of ellipsoidal forms of our nanovoids (Fig. 9). This macroscopic model allows explaining basic peculiarities of experimental data of Fig. 9.

The creation of five groups of nanovoids (Fig. 9c) is caused of "moving" focuses in irradiated matter, which is connecting with processes of blooming at the irradiation time [42].

Thus for the explanation laser-induced volume phase transformations we must use models of laser-induced breakdown, moving focuses, radiation physics of status solid and shock waves.

V. Conclusions

1. Problems of modeling the phase transformations Relaxed Optics are analyzed.
2. Some experimental data of creation the laser-induced phase transformations in solid are observed.
3. Short comparative analysis of basic theories and methods of modeling phase transitions and phase transformations is discussed.
4. Cascade model of excitation of proper chemical bonds in the regime of saturation the excitation was used for the explanation the represented experimental data for the laser-induced surface phase transformations.
5. Elements of the models of moving focuses, radiation physics of status solid, laser-induced breakdown and shock waves are used for the explanation of basic peculiarities of volume laser-induced phase transformations.

REFERENCES

[1]. H. Haken, Synergetics, Moscow, Russia: Mir, 1980. (In Russian)
[2]. P. P. Trokhimchuck, Nonlinear and Relaxed Optical Processes. Problems of Interactions, Lutsk, Ukraine: Vezha-Print, 2013.
[3]. P. P. Trokhimchuck, "Relaxed Optics: Necessity of Creation and Problems of Development," Int. J. Adv. Res. Phys. Sc. (IJARPS), vol. 2, is. 3, pp. 22-33, Murch, 2015.
[4]. P. P. Trokhimchuck, Relaxed Optics: Realities and Perspectives, Saarbrukken, Germany, Lambert Academic Press, 2016.
[5]. A.V. Andreev, V. I. Emelyanov and Yu. A. Ilyinskiy, Cooperative phenomena in optics, Moscow,USSR: 1988. (In Russian)
[6]. P. P. Trokhimchuck, Theoretical Physics. Lutsk, Ukraine: Vezha-Print, 2017. (In Ukrainian)
[7]. G. Careri, Order and Disorder in Matter, New York, USA: Benjamin/Cummings Inc., 1984.
[8]. Ye. M. Lifshitz', "To the theory of critical phenomena," Journal of experimental and theoretical physics, vol. 11, is.2-3, pp. 255-281, Feb.-Murch, 1941 (In Russian)
[9]. R. A. Cowley and A. D. Bruce, "The theory of structurally incommensurate systems. I. Disordered-incommensurate phase transitions," J. Phys.C., vol. 11, is. 17, pp. 3577-3590, 1978.
[10]. R. A. Cowley, A. D. Bruce and A. F. Murray, "The theory of structurally incommensurate systems. II. Commensurate-incommensurate phase transitions," J. Phys.C., vol. 11, is. 17, pp. 3591-3608, 1978.
[11]. R. A. Cowley and A. D. Bruce, "The theory of structurally incommensurate systems. III. The fluctuations spectrum of the incommensurate phases," J. Phys.C., vol. 11, is. 17, pp. 3608-3630, 1978.
[12]. Topological Phase Transitions and Topological Phases of Matter. Scientific Background of the Nobel Prize, Stokholm, Sweden: The Royal Swedish Academy of Sciences, 2016.
[13]. R. Ya. Holovchak, Structural-topological Self-organization of Networks Systems of Chalcohenide Glasses. D. Sc. Thesis, Lviv, Ukraine: Orest Vlokh Insitute of Physical Optics, 2016. (In Ukrainian)
[14]. P. P. Trokhimchuck, Continuum Mechanics, Lutsk, Ukraine: Vezha-Print, 2018. (In Ukrainian)
[15]. P. P. Trokhimchuck, "Problem of saturation of excitation in Relaxed Optics," Journal of Optoelectronics and Advanced Materials, vol. 14, is.2-3, pp. 363–370, 2012.
[16]. P. P. Trokhimchuck, Nonlinear Dynamical Systems, Lutsk, Ukraine: Vezha-Print, 2015. (In Ukrainian)
[17]. L. de Broglie, "Thermodynamics of isolated point (Hidden thermodynamics of particles)," in L. de Broglie. Collected papers, vol. 4, Moscow, Russia: Print-Atel'e, pp. 8 – 111, 2014 (In Russian)
[18]. M. Birnbaum, "Semiconductor surface damage produced by Ruby Laser," J. Appl. Phys., vol. 36, is.11, pp. 3688–3689, 1965.
[19]. B. S. Sharma, Laser-induced dielectric breakdown and mechanical damage in silicate glasses. Ph. D. Thesis, Burnaby, Canada: Simon Fraser University, 1968.
[20]. A. Medvid', "A. Nano-cones Formed on a Surface of Semiconductors by Laser Radiation," in Technology Model and Properties. Nanowires Science and Technology, ed. Nicoletta Lupu, Vucovar, Croatia: Inech, pp. 61–82, 2010.
[21]. A. J. Pedraza, J. D. Fowlkes and D. H. Lowndes, "Silicon microcolumn arrays growth by nanosecond pulse laser irradiation," Appl. Phys. Lett., vol. 74, is. 10, pp. 2222-2224, 1999.
[22]. A. J. Pedraza, Y. F. Guan, J. D. Fowlkes, D. A. Smith and D. H. Lowndes, "Nanostructures produced by ultraviolet laser irradiation of silicon. I. Rippled structures," J. Vac. Sc. @ Techn. B., vol. 22, is. 10, pp. 2823-2835, 2004.
[23]. M. Shen, J. E. Carey, C. H.Crouch, M. Kandyla, H. A. Stone and E. Mazur, "High-density regular arrays of nano-scale rods formed on silicon surfaces via femtosecond laser irradiation in water," Nanoletters, vol. 8, is. 7, pp. 2087-2091, 2008.
[24]. Makin V.S. Regularities of creation of ordering micro- and nanostructures in condensed matter for laser excitation of mode of surface polaritons. D.Sc. Thesis, Saint-Petersburg, Russia: State University of Informative Technologies, Mechanics and Optics, 2013. (In Russian)
[25]. P. P. Trokhimchuck, "Problems of modeling the creation the surface laser-induced structures in Relaxed Optics," Bulletin of Karazin Kharkiv National University. Physics, vol. 27, pp. 35 – 43, 2017.
[26]. P. P. Trokhimchuck, "About the mechanisms of the formation of surface laser-induced structures," Journal of the Belorussian State University. Physics, is. 1, pp. 58 – 65, 2018. (In Russian)
[27]. M. Tsukamoto, K. Asuka, N. Nakano, M. Hashida, M. Ratto, N. Abe and M. Fujita, "Period microstructures produced by femtosecond laser irradiation on titanium plate," Vacuum, vol. 80, pp. 1346-1350, 2006.
[28]. T. Okada, T. Tomita, S. Matsuo, S. Hashimoto, R. Kashino and T. Ito, "Formation of nanovoids in femtosecond laser irradiated single crystal silicon carbide," Material Science Forum, is. 725, pp. 19 – 22, 2012.

[29]. T. Okada, T. Tomita, S. Matsuo, S. Hashimoto, Y. Ishida, S. Kiyama and T. Takahashi, F"ormation of periodic strain layers associated with nanovoids inside a silicon carbide single crystal induced by femtosecond laser irradiation," J. Appl. Phys., vol. 106, is 5, 054307, pp. 5, 2009.
[30]. Ya. Tauc, "Optical properties of semiconductors in visible and ultraviolet ranges," Uspekhi fizicheskikh nauk, vol. 94, is. 3, pp. 501 – 533, 1968. (In Russian)
[31]. J.C. Philips, "Metastable honeycomb model of laser annealing," J. Appl. Phys., vol. 52, is. 12, pp. 7397-7402, 1981.
[32]. P. P. Trokhimchuck, Radiation Physics of Status Solid, Lutsk, Ukraine: Vezha, 2007. (In Ukrainian)
[33]. S. Chandrasekar, Hydrodynamic and Hydromagnetic Stability, New York, USA: Dover Publications, 1961.
[34]. M. J. Donachie, Titanium: A Technical Guide, Ohio, USA: Materials Park, 2000.
[35]. P. P. Trokhimchuck, "Problems of reradiation and reabsorption in Nonlinear and Relaxed Optics t," Int. J. Adv. Res. Phys. Sc. (IJARPS), vol. 4, is. 2, pp. 37-50, Feb., 2017.
[36]. Ki-Taek Byun and Ho-Young Kwak, "A model of laser-induced cavitation," Jap. J. Appl. Phys., vol. 43, is. 2, pp. 621-630, .2004.
[37]. T. Juhash, G. A. Kastis, C. Suares, Z. Bor, and W. E. Bron "Time-Resolved Observations of Shock Waves and Cavitation Bubbles Generated by Femtosecond Laser Pulses in Corneal Tissue and Water," Lasers in Surgery and Medicine, vol. 19, pp. 23 – 31, 1996.
[38]. W.Lauteborn and T. Kurz, "Physics of bubble oscillations," Rep. Progr. Phys., vol. 77, 106501, pp. 88, 2010.
[39]. F.V. Potemkin and E. I. Mareev, "Shock waves and cavitation bubbles dynamics as a function of the tightly focused femtosecond laser energy in distilled water and acetone," Scientific Notes of Physical Faculty. Mikhail Lomonosov Moscow State University, 133401, pp. 9, 2013 (In Russian)
[40]. S. M. Ryndya, Peculiarities of Thin Films SiC structure, which is formatted on Si and Al_2O_3 substrates by method of pulse laser precipitation. Ph. D. Thesis, Moscow, Russia: L. Ya Karpov Scintific Research Physica-Chemical Institute, 2014. (In Russian)
[41]. D. O. Moskovskikh, Production of Submicrometer Powder of Silicon Carbide and Nanostructural Ceramics on its Basis. Ph. D. Thesis, Moscow, Russia: National Research Technological University of Steel and Alloys, 2015. (In Russian)
[42]. Self-Focusing: Past and Present. Eds. R.W. Boyd, S.G. Lukishova, Y.-R. Shen, Springer Series: Topics in Applied Physics, Vol. 114, Berlin, Germany: Springer, 2009.

Petro P. Trokhimchuck " Problems of Modeling the Phase Transformations in Nonlinear and Relaxed Optics" International Journal Of Engineering Research And Development , vol. 14, no. 02, 2018, pp. 48–61.